🏆 *reviewed paper*

A Suite of Novel EO-Based Products in Support of Urban Green Planning

Mattia Marconcini, Annekatrin Metz

(Dr. Mattia Marconcini, German Aerospace Center, Wessling, Germany, mattia.marconcini@dlr.de)
(Annekatrin Metz, German Aerospace Center, Wessling, Germany, annekatrin.metz@dlr.de)

1 ABSTRACT

The strategic implementation of green infrastructures can sensibly help facing the effects of climate change in urban areas by reducing high temperatures, decreasing stormwater runoff, saving energy, improving air quality and increasing biodiversity. In this framework, the benefits of green roofs and urban trees are many and well documented in several recent studies, hence their monitoring is of high use for urban planners to properly design effective adaptation and mitigation strategies. Nevertheless, such activities have been so far solely carried out by means of in situ surveys or photointerpretation of very high resolution airborne imagery, thus being very costly both in terms of money and time. To overcome this drawback, we implemented two novel techniques aimed at automatically identifying current and potential green roofs, as well as mapping tree location and canopy, respectively. In particular, this is carried out by jointly exploiting satellite/airborne color infrared remote sensing imagery and LiDAR height data. Experimental results obtained for Antwerp, Milan, the Helsinki Capital Region, and the Royal Borough of Kensington and Chelsea assess the effectiveness and potential of the proposed techniques.

2 INTRODUCTION

Climate change poses serious challenges to urban areas affecting different sectors of the city life; accordingly, decision makers need to implement suitable plans to effectively lessen its negative effects. In this framework, maintaining and increasing urban green areas is of great importance for many reasons like reducing stormwater runoff (which transports toxic chemicals, dirt and trash from roofs and roads into lakes, streams and rivers but also leads to an increased occurrence of urban flooding events), lowering air pollution (which is responsible for a variety of respiratory and cardiovascular conditions) and mitigating the urban heat island effect (which causes high-energy consumption for cooling and an increase of heat-related illness and fatalities). Furthermore, green areas enable biodiversity and the conservation of several species and enhance the wellbeing and quality of life of urban residents. In such scenario, we present a suite of novel Earth Observation (EO) based products developed for supporting urban managers to improve their urban green planning strategies. In particular, this includes key information about green roofs and trees derived from very high resolution satellite/airborne color infrared (CIR) remote sensing imagery and LiDAR height data.

On the one hand, green roofs are gaining increasing attention as a versatile new environmental mitigation technology (Oberndorfer et al., 2007; Ansel and Appl, 2009). In particular, they exhibit several advantages like:

- absorbing rainwater: the installation of a green roof can significantly improve rainwater quantity and quality, hence reducing the stormwater runoff (through membrane absorption and plant evapotranspiration) which can have a significant impact on natural environments as well as sewage conveyance given the presence of pollutants and suspended solids in the water (VanWoert et al., 2005; Ansel and Diem, 2009; Berndtsson 2010);

- providing thermal insulation: in summer, a green roof not only acts as an insulation barrier, but the combination of plant and soil processes reduces the amount of solar energy absorbed by the roof membrane, thus leading to cooler temperatures beneath the surface; in winter, green roofs can help to reduce heat loss from buildings when root activity of plants, air layers and the totality of the specific system create heat and thereby provide an insulation membrane (Liu and Baskaran, 2003; Hui 2009; Gall et al., 2010);

- increasing energy efficiency: the greater insulation offered by green roofs can reduce the amount of energy needed to moderate the temperature of a building, as roofs are the sight of the greatest heat loss in the winter and the hottest temperatures in the summer. For example, research published by the National Research Council of Canada found that a green roof can reduce the daily energy demand for air conditioning in the summer by over 75% (Liu and Baskaran, 2003);

- reducing air pollution: green roofs contribute to the reduction of a number of polluting air particles and compounds not only through the plants themselves, but also by deposition in the growing medium itself; therefore, being absorbed into the green roof system these polluting particles do not enter the water system through surface run off leading to improvement in water quality (Yang et al., 2008; Rowe 2011);

- reducing electromagnetic radiation: the risk posed by electromagnetic radiation (from wireless devices and mobile communication) to human health is still a question for debate; nonetheless, green roofs are capable of reducing electromagnetic radiation penetration by 99.4% (Herman 2003);

- reducing noise: green roofs have excellent noise attenuation, especially for low frequency sounds; in particular they can reduce sound from outside by 40-50 decibels (Peck et al., 1999).

In this context, mapping green roofs is then of high importance; moreover, being their installation usually supported by subsidies, a precise identification of their location is of great help (also to properly plan activities for checking their actual status). Nevertheless, green roof identification is presently extremely costly and time demanding being it mostly carried out by photointerpretation of airborne imagery or in situ surveys by experts. To overcome this limitation, we implemented a novel method which allows to automatically identify actual green roofs and determining which roofs can be potentially converted into green roofs along with the corresponding expected impact (which is of valuable support to target subventions in areas which would more benefit from this change). Specifically, by analyzing the slope computed from the height data, we first identify flat roofs. Among these, we then mark as green those exhibiting consistent vegetation coverage using the normalized difference vegetation index (NDVI) computed from the CIR imagery. All the remaining are denoted as potential green roofs and their impact is finally estimated by taking into account the local surface imperviousness. The support of an operator is mainly requested only at the end of the processing chain to visually check the results and exclude roofs falsely identified as green roofs due to intrinsic limitations of the input data used. This represents a great advantage with respect to current approaches (i.e., lower costs and shorter time) and also allows an easy and straightforward update once provided with new suitable imagery.

On the other hand, in several cities it occurs that no or incomplete trees inventories (e.g., just including public ones) are available directly at the municipality. However, this source of information is of high importance being trees capable of absorbing carbon dioxide while releasing oxigen back into the air, cooling the cities by shading, reducing runoff by breaking rainfall, as well as providing habitat to wildlife. Furthermore, an exhaustive tree register allows to identify where there is a higher need for planting new ones and enhances the ability to educate the public and decision makers about their importance as well as the need to care for and protect them. Presently, tree records are generally compiled via in situ surveys (often by volunteers) which require plenty of time. In the literature, only few techniques have been presented so far to address this task, which are mostly based on Geographic Object Based Image Analysis (GEOBIA) applied to satellite CIR imagery (Karlson et al., 2014). Nevertheless, the lacking of height information results in poor performances. To tackle this issue, we developed an automatic technique that allows to routinely create a reliable map of the tree location and of their canopy in a given study area. In particular, all the vegetated areas are first identified by the analyis of the NDVI calculated from the CIR data; then, the tree canopy is delineated accounting for the height information and finally a tree location is set in correspondence of the highest peak of its crown.

The whole suite of presented products has been developed within the FP7 DECUMANUS (DEvelopment and Consolidation of geo-spatial sUstainability services for adaptation and environmental and cliMAte chaNge Urban impactS) project. In particular, DECUMANUS had the principal objective to develop and consolidate a set of sustainable services that allows city managers to incorporate EO-based geo-spatial products and geo-information services in their climate and environmental change strategies to support the sustainable management of the cities in Europe. In the following, the two corresponding services will be described into details, namely current and potential green roof mapping and tree location and canopy mapping, respectively. Experimental activities in cooperation with the DECUMANUS partner cities of Antwerp, Milan, the Helsinki Capital Region (including the cities of Helsinki, Espoo, Vantaa and Kauniainen), and the Royal Borough of Kensington and Chelsea (RBKC) assess the accuracy of the developed products and confirm their great potential for supporting climate change mitigation strategies.
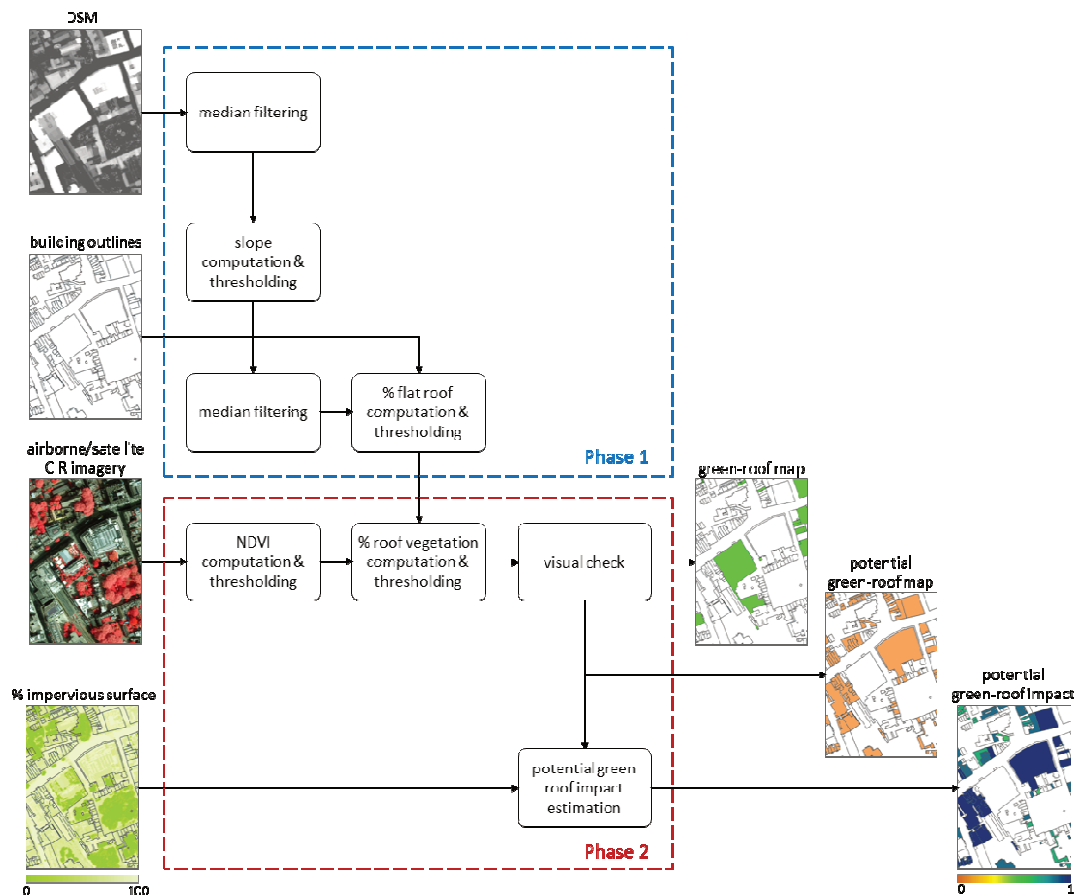
Fig. 1: Block scheme depicting the algorithm developed for mapping both current and potential green roofs.

3 CURRENT AND POTENTIAL GREEN ROOF MAPPING

A block scheme depicting the algorithm designed for mapping both current and potential green roofs is provided in Fig. 1. In particular, the developed technique improves the one originally implemented at the German Aerospace Center (DLR) in cooperation with the German Roof Gardener Association (DDV) in the context of the project "Remote Sensing: Green Roof Inventory and Potential Analysis" financed by the German Federal Environmental Foundation (DBU) (Zeidler et al., 2015).

For a given area of interest, the requested input data are:

- Digital Surface Model (DSM): raster file where each pixel is associated with the elevation above the sea level of the corresponding ground or any feature on it (hence also including buildings and trees);
- building outlines: vector file solely including building types which are suitable for hosting a green roof according with the specific policies of the city under investigation (e.g., underground garages covered by gardens in Milan are still considered as green roofs, while this is not true for Antwerp);
- CIR imagery [either airborne or satellite]: raster file including one band acquired in the near infra-red (NIR) and one in the red portion of the electromagnetic spectrum;
- imperviousness map: raster file where each pixel is associated with the (percentage) amount of the corresponding surface covered by paved structures [also available as DECUMANUS service (Marconcini et al., 2015)].

In order to properly characterize small structures as building roofs, both the above-mentioned DSM and CIR imagery have to be provided at very high resolution (VHR). Specifically, the most suitable range proved to be between 25cm and 2m. Indeed, for resolutions finer than 25cm the computational load generally becomes extremely high without bringing any significant benefit; instead, at resolutions coarser than 2m most of the roofs cannot be correctly identified. As regards the imperviousness map, since (as it will be clarified next) its average is computed for each building within a buffer around its outline, a spatial resolution up to some tens

of meters is acceptable [e.g., the percentage imperviousness map generated in the context of DECUMANUS by means of Landsat imagery at 30m spatial resolution (Marconcini et al., 2015)].

Fig. 2: Current and potential green roof maps obtained with the presented technique overlaid to the available CIR airborne imagery for a subset of the Antwerp (top left) and Helsinki (top right) study areas, along with the corresponding potential green roof impact maps (bottom left) and (bottom right), respectively.

The implemented methodology is structured in two phases: Phase 1 is dedicated to identifying those roofs where at least a significant portion is flat enough to host (or potentially host) a green roof; Phase 2 aims at assessing the portion of the roofs identified in Phase 1 covered by vegetation and generating the intended products, namely the green roof map, potential green roof map, and potential green roof impact. In the following each of them is described into details.

3.1 Phase 1

As the DSM is mostly derived from LiDAR airborne acquisitions, it is often affected by speckle (granular) noise. To overcome this issue, a common but effective approach is to employ a median filter which generally allows to remove the noise while preserving the edges of different objects. Since we are dealing with VHR data, based on extensive empirical analysis a reasonable choice proved to be a median filter of size 3x3 pixels. Afterwards, for each pixel of the filtered DSM we compute the slope, defined as the maximum rate of elevation between the given pixel and its neighbors. Flat (or quasi-flat) roofs are the ones more suitable for installing a green roof. Accordingly, a binary mask is derived based on a prefixed threshold σ on the slope

(which is set by default to 12☐ but might vary depending on specific city policies/ requirements, e.g. 15☐ was requested by the city of Antwerp) and then filtered again by means of a 3x3 median filter in order to remove single pixel objects or fill single-pixel gaps. Next, based on the resulting mask we compute for each building the corresponding percentage of flat surface. A vector file is finally generated solely including the roofs whose flat surface percentage is greater than 10% if their size is lower than 100 m² or greater than 5% if their size is greater than 100 m², which are those considered as suitable for hosting a green roof (this ruleset generally proved to be rather effective; nevertheless, it can easily be tuned according to the specific needs of the final users).

3.2 Phase 2

By means of the NIR and red bands of the available CIR imagery, we compute the NDVI which ranges from -1 to +1 and is used in a variety of remote-sensing applications to assess for each pixel the amount of live green vegetation present in the corresponding portion of the surface (Rouse et al., 1974). Here, the idea is to derive a binary mask based on a threshold η on the NDVI where pixels exhibiting values higher than η are associated with vegetated areas. However, the NDVI strongly depends on the specific time of the year when the CIR imagery has been acquired, as well as from the geographical location of the city under investigation. Accordingly, it is not possible to set a priori a reliable threshold η but simply an operator has to manually derive it. In particular, the value is determined as the minimum NDVI computed for a certain amount of pixels (generally few tens are sufficient) extracted throughout the entire study site from areas covered by grass (i.e., where the NDVI is lower compared to areas covered by bushes or trees). Then, based on the resulting mask, for each of the buildings identified as suitable for hosting a green roof obtained at the end of Phase 1 we compute the corresponding percentage of surface covered by vegetation.

Two vector files are finally generated: one includes the estimated green roofs defined as those whose percentage vegetation cover is greater than 10%; the other includes all the remaining (whose percentage vegetation cover is lower or equal to 10%), hence corresponding to the estimated potential green roofs. It is worth pointing out that in this case selecting 10% as a threshold results in a slight overestimation of the green roofs. Nevertheless, being anyhow a visual check mandatory to deal with challenges posed by the data themselves (as clarified in Section 4), it is preferable to avoid any false detection and to manually exclude roofs falsely identified as green roofs (which are then merged to the estimated potential green roofs). Indeed, while the total number of buildings for the 4 cities investigated in the context of DECUMANUS is of the order of tens/hundreds of thousands, the number of automatically estimated green roofs is generally of some few thousands. Accordingly, it is evident the big improvement with respect to current practices where the entire analysis is carried out by photointerpretation. The refined layers obtained after the visual post-processing delineate the final green roof and potential green roof maps.
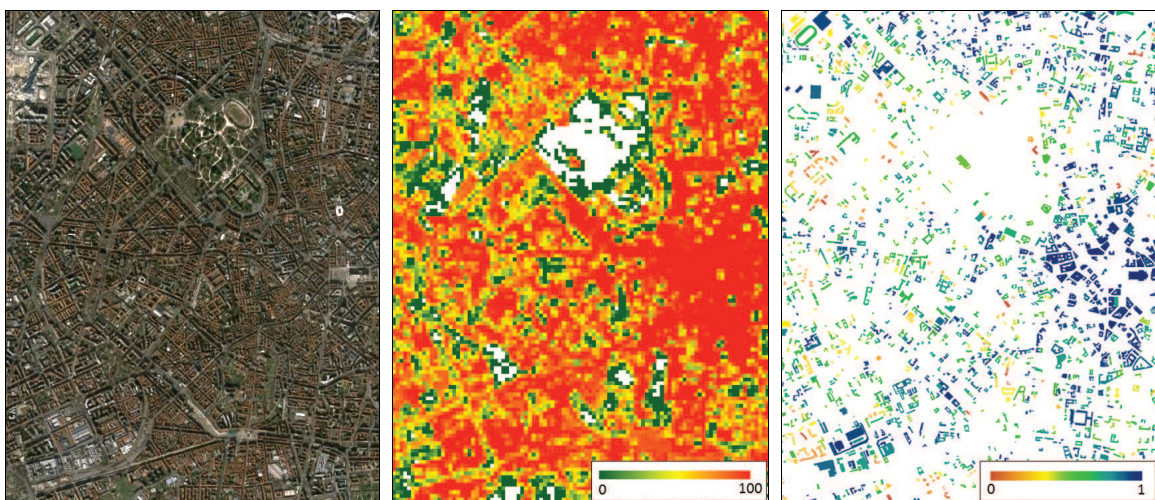

Fig. 3: Milan – GoogleEarth imagery of a subset of the study area including the city center (left), along with the corresponding percentage imperviousness map generated in the context of the DECUMANUS project (middle), and the potential green roof impact map generated by means of the presented approach (right).

It is important to highlight that not all the identified potential green roofs might have the chance to be actually converted into real green roofs. In fact, they also need to fulfill the structural requirements for the

load necessary to mount a green roof (while newly constructed buildings should meet them, this might not be true for older constructions). Nonetheless, such type of information cannot be retrieved from any remote-sensing data, but exclusively via in situ survey.
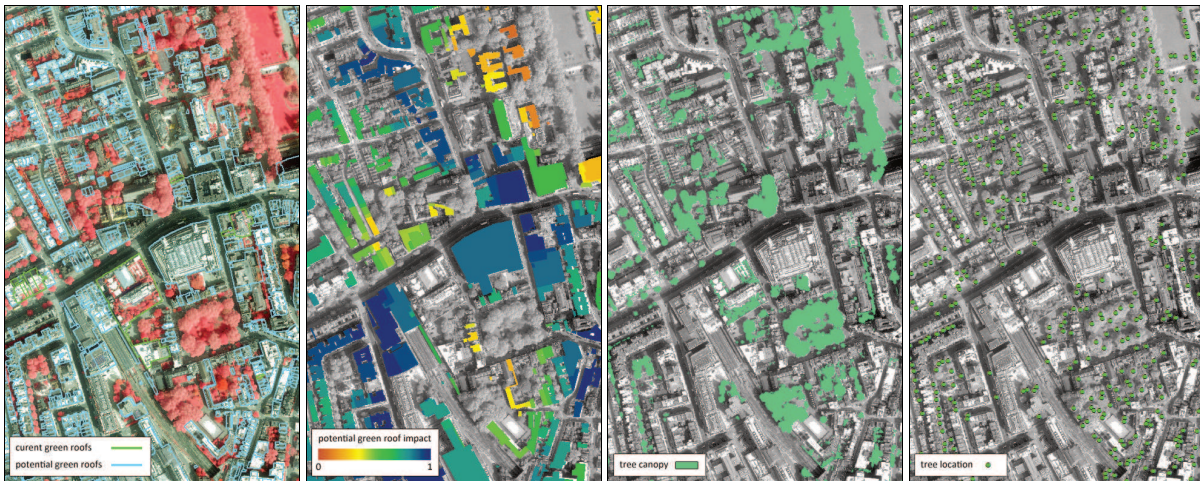

Fig. 4: RBKC – Current and potential green roof maps obtained with the presented technique overlaid to the available CIR airborne imagery (a), estimated potential green roof impact (b), tree canopy coverage (c), and tree locations (d) derived with the proposed methodologies.

Finally, it is intuitive that installing a new green roof in an area with a high local imperviousness is expected to be more beneficial to the whole urban environment than installing a green roof in a rural area yet characterized by a consistent presence of vegetation in the surroundings. Accordingly, as a means for estimating their impact, we compute for each potential green roof the average percentage imperviousness within a buffer of 100m outside its outline. The output is rescaled between 0 and 1, where 0 corresponds to "no effect", and "1" to "maximum effect".

3.3 Experimental Results

The above-mentioned green roofs maps have been produced for the 4 listed DECUMANUS partner cities. In particular, CIR airborne imagery was available for Antwerp, the Helsinki Capital Region and the RBKC at 25-50cm spatial resolution, while for Milan WorldView-3 satellite data at 1.2m spatial resolution have been employed. LiDAR-based DSM layers at 50cm/1m resolution were available for all the study areas. Examples of the final products are reported in Fig. 2 for a subset of the Antwerp and Helsinki areas of interests. Moreover, in Fig. 3 GoogleEarth imagery of a subset of the Milan study site including the city center is shown, along with the corresponding percentage imperviousness map generated in the context of the DECUMANUS project (Marconcini et al., 2015), and the resulting potential green roof impact map. Results for a portion of the RBKC are also given in Fig. 4 a-b.

It is worth pointing out that for all the investigated cities no green roof database is available for comparison, being their growing employment a new trend occurring only very recently. Instead, the outcomes of the proposed methods are intended to be used as first reference layers by the municipalities. The main idea of the described method is to avoid missed alarms while setting an NDVI threshold which results in a low amount of false alarms to be refined in the post-processing visual check. This last step also aims at overcoming the issues related to the specific available data as described in Section 4. In this framework, we expect the final output products to be correct with, in case, negligible over and underestimation (indeed, any identified error is properly corrected in the post processing). This has also been confirmed by the highly satisfactory feedback received from the users.

4 TREE LOCATION AND CANOPY MAPPING

A block scheme depicting the algorithm developed for mapping tree location and their canopy is reported in Fig. 5. As one can notice, in addition to DSM, building outlines and VHR CIR airborne/satellite imagery for the area under investigation (also used for deriving the green roof products), the corresponding Digital Terrain Model (DTM) needs to be provided as input too. In particular, the DTM is a raster file where each pixel is associated with the elevation above the sea level of the corresponding ground (hence – contrarily to the DSM – not including buildings or trees).
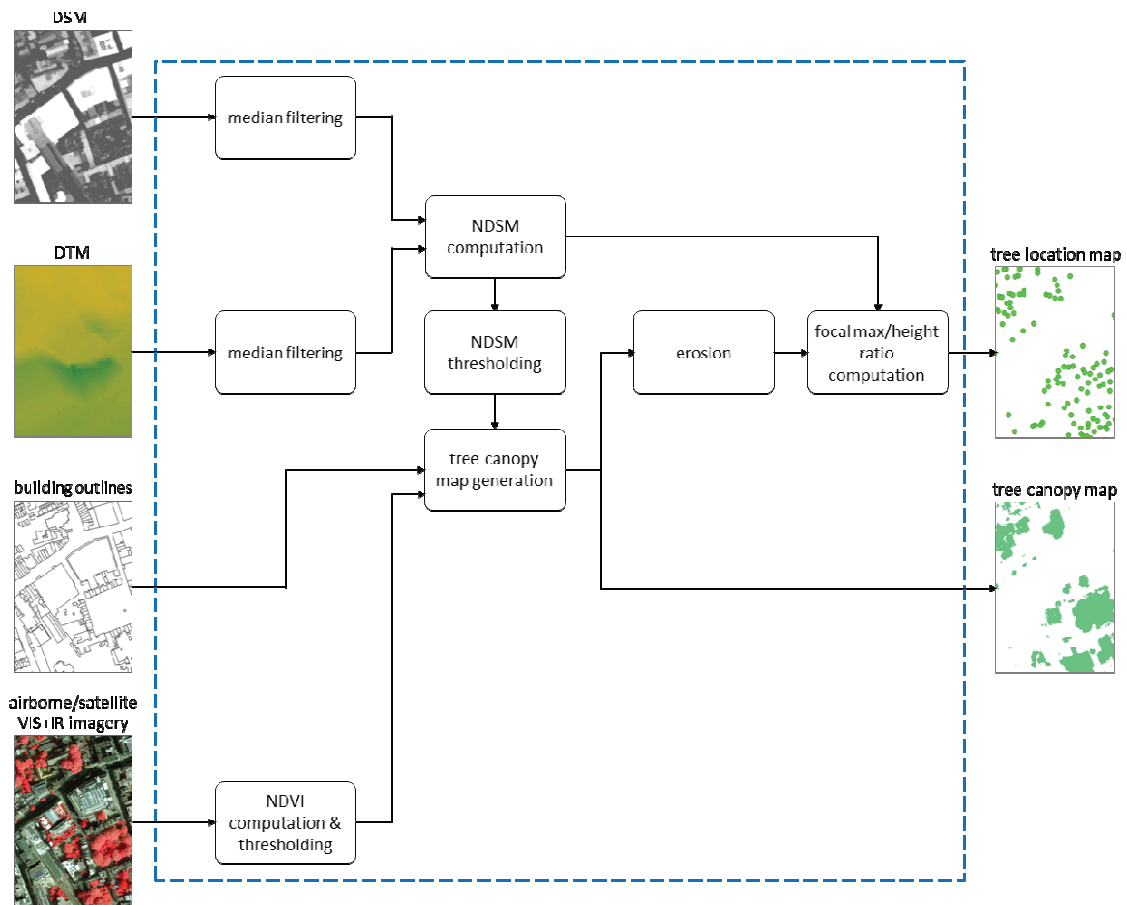
Fig. 5: Block scheme depicting the algorithm developed for mapping tree location and their canopies.

To properly calculate the relative height of an object with respect to the ground, we compute the so-called normalized DSM (nDSM), which is given by the difference between the available DSM and DTM. As described in the previous section, to remove the speckle (granular) noise affecting the DSM and DTM, we first apply to both a median filter of size 3x3 pixels. A binary mask is then derived from the nDSM, where all the pixels whose relative height is lower than 2m and those whose relative height is equal or greater than 2m are associated with different values, respectively. In parallel, as done for mapping current and potential green roofs, we compute the NDVI from the available CIR imagery and derive from it a binary mask where pixels higher than the threshold η are associated with vegetated areas. Since the NDVI strongly depends on the geographical location of the study area, as well as the specific time of the year when the CIR imagery has been acquired, here the value of η is determined as the minimum NDVI computed for some tens of pixels manually extracted from random tree crowns. The resulting mask is further combined with both the available building outlines and the above-mentioned nDSM-based mask. In particular, only the vegetated pixels outside the building outlines whose relative height is equal or greater than 2m are kept (indeed, after consulting with the DECUMANUS users it has been agreed that vegetation lower than 2m shall never be categorized as "tree"). The output exactly corresponds then to the tree canopy map.

In general, the position of a trunk can be reasonably set to the pixel where its crown has the maximum height. Therefore, in order to derive the intended tree location map, the idea is to identify local maxima in the nDSM within the areas delineated as tree crowns. To this purpose, we first apply an erosion filter (of 1 pixel size) which allows to slightly simplify the geometry at the borders of the objects marked as canopies. Next, we mask the nDSM with the obtained layer and employ a focal maximum filter which computes for each pixel the maximum height among its neighbors within a circle of pre-defined size. In particular, we assume that on average the tree crown diameter is of the order of 3.5m within urban areas, hence we set the filter size accordingly based on the nDSM spatial resolution (e.g., for an nDSM of 50cm spatial resolution a circle of 7 pixels diameter is used). Finally, we divide the output of the focal maximum filtering by the nDSM. Pixels exhibiting a ratio equal to 1 (i.e., those whose height coincides with the maximum within the considered circle) are the intended local maxima and are set as the tree location sites.
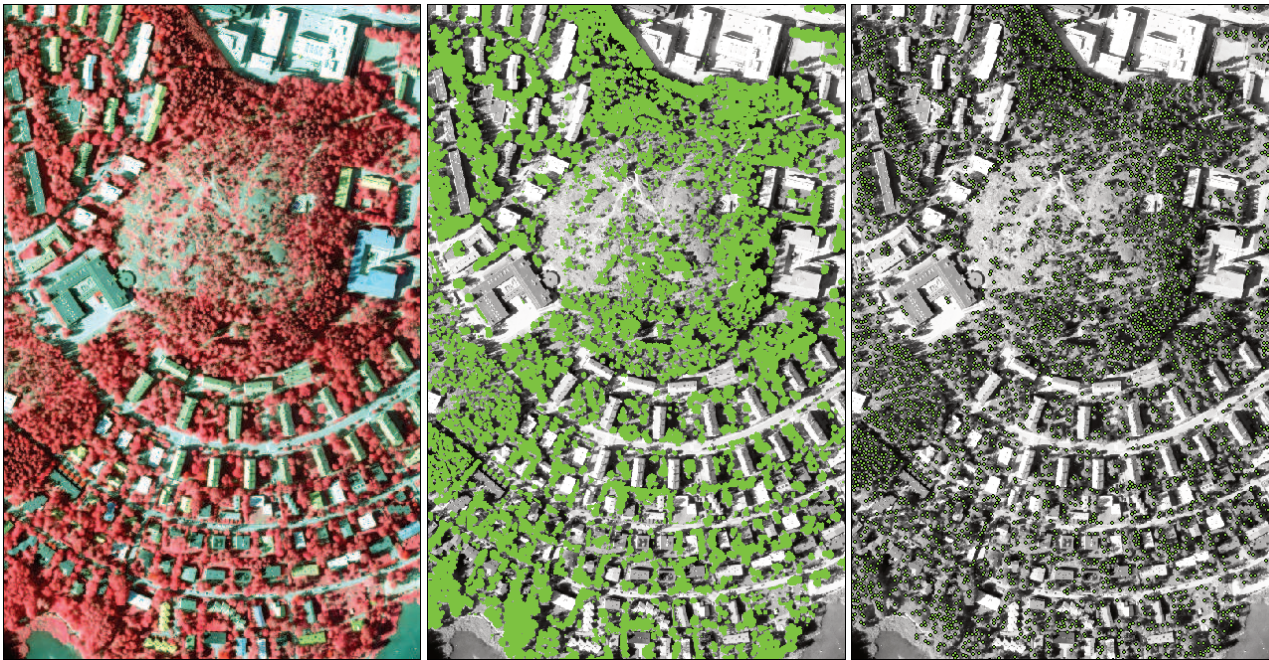
Fig. 6: Helsinki – available CIR airborne imagery for a subset of the study area (left), along with the corresponding tree canopy map (middle) and tree location map (right) derived with the presented technique.

4.1 Experimental Results

Basd on the DECUMANUS user requirements, the tree location and canopy maps have been produced for the Helsinki Capital Region and the RBKC. The data used are the same employed for deriving the green roof maps described in Section 3 with the addition of LiDAR-based DTM available in both cases at 50cm spatial resolution. An example depicting a portion of the final products derived for the RBKC is given in Fig. 4 c-d. Moreover, in Fig. 6 the available CIR airborne imagery for a subset of the Helsinki study area is reported, along with the corresponding tree canopy and tree location maps. In both cases, the proposed algorithm proved to be very accurate and allowed to obtain extremely reliable products. To quantitatively assess their effectiveness, we performed two different types of validation analyses. As regards the tree canopy map, we randomly subsampled 3000 pixels from those categorized as canopies and 3000 pixels from all the remaining; then, we visually checked their labels and finally compared it to that automatically associated by the presented method. Both for the RBKC and Helsinki, we obtained an overall accuracy higher than 98%. Instead, concerning the tree location map, we compared the obtained final product against the location of 3000 trees manually selected within the study area by photointerpretation; moreover, we randomly selected 3000 among the trees identified by the presented technique and visually assessed whether a tree was actually present nearby. In both cases, we allowed a tolerance of 2m between the estimated and actual location of the trees. Also in this case the obtained performances are highly satisfactory, with overall accuracies higher than 95% for both the RBKC and Helsinki. False alarms are very unlikely, whereas missed alarms are few and mostly occur in the presence of clusters where several trees are very close to each other (where even by photointerpretation it is tough to reliably understand how many trees are present).

5   DISCUSSION AND CONCLUSION

As confirmed by the very positive feedback from the municipalities of the DECUMANS city partners, the EO-based products derived by applying the proposed techniques are very effective and reliable. However, some limitations might occur mostly due to the specific EO data employed, but also to the lack of clear common definitions. In this context, a summary is given below on the basis of the performed extensive experimental analysis.

Definition of green roof: Presently, there is not a common agreed green roof definition at the European level, but rather each country or municipality has its own specific guidelines. As an example, in some cities all vegetation layers on top of any construction are basically considered as green roofs (thus also including underground garages with gardens at the ground level on top of them), while in some others underground garages are excluded from the green roof count. Accordingly, the provided building outlines shall include the

information necessary to exclude from the analysis all those roofs which do not match the criteria for the specific investigated city. In case this is not available, additional resources are needed in the post-processing phase to manually overcome the resulting overestimations.

Definition of tree: despite the term "tree" is of regular use in everyday life, actually there is no common agreed definition of what a tree is, either botanically or in common language. Broadly speaking, a tree is any plant with the general form of a single elongated stem (or, in case, of coppice several stems), or trunk, which supports the photosynthetic leaves or branches at some distance above the ground (Gschwantner et al., 2009). In our case we assumed it to be 2m; however, this value might be changed depending on the specific requirements from the end users.

Green roof type: green roofs are categorized either as intensive or extensive. Intensive green roofs are characterized by deep substrates and a variety of plantings and have the appearance of conventional ground-level gardens (Oberndorfer et al., 2007); in particular, they mostly include perennials, lawn, putting green, shrubs and trees. Instead, extensive green roofs have shallower substrates, require less maintenance, and are more strictly functional in purpose than intensive green roofs (which are often used as leisure roof gardens). In their simplest design, extensive green roofs consist of an insulation layer, a waterproofing membrane, a layer of growing medium, and a vegetation layer (Oberndorfer et al., 2007) typically composed of mosses, sedums, succulents, herbs or grasses. Intensive green roofs are easier to identify as they are normally characterized by high NDVI values, whereas extensive green roofs generally exhibit lower NDVI, hence being more difficult to recognize. Accordingly, it is important to properly set an NDVI threshold that allows to avoid missed alarms.

Actuality of data: DSM, DTM, CIR imagery and building outlines should refer to times as close as possible. If this does not occur, then both under and over estimation might occur. In case demolished buildings are not erased from the databse, they often result in overestimations due to the appearance of natural vegetation, thus requiring more efforts in the post-processing visual check.

CIR imagery acquisition time: the NDVI has an ascending trend from the beginning to the peak of the growing season (in correspondence of which it exhibits its minimum and maximum, respectively); then, it gradually decreases again to its minimum at the end of the growing season. Typically the growing season starts in April and ends around October/November; however, it strongly varies with the altitude and latitude. For instance, in the alpine region and in Northern Europe it spans from June to September, whereas in Spain and Portugal it is almost year-round. The closer is the available CIR imagery to the peak of the growing season for the specific study area, the better are the expected performances of the presented methods. In general, June and July acquisitions are ideal. For acquisitions taken in March or September it might be not feasible to properly identify extensive green roofs due to the corresponding very low NDVI value; moreover the absence of leaves might also prevent detecting deciduous tree species.

CIR imagery spatial resolution: the higher is the spatial resolution, the more are the details which can be recognized. Accordingly, airborne imagery is preferred as its spatial resolution is typically of the order of few tens of centimeters; nevertheless, it is generally very costly. Alternatively, VHR satellite imagery can be employed with spatial resolutions between 1 and 2m. In this case, costs are sensibly lower; however, the coarser resolution might result in some underestimations of smaller trees/green roofs that can be solely correct by visual check, hence requiring longer post-processing working time. Ideally, to avoid discrepancies, the available DSM/DTM should have the same spatial resolution of the CIR imagery.

CIR imagery viewing angle: the viewing angle at which the CIR imagery is acquired is one of the key factors especially for the green roof mapping. Indeed, the lower it is, the more critical are the shadowing effects and the misalignment of the higher buildings with respect to the available outlines. In the former case, green roofs falling in shadowed areas due to higher buildings in the surroundings cannot be identified (not even by means of post-processing corrections). In the latter case, the higher is one building, the greater is the shift of the corresponding outlines (which can result either in underestimations or overestimations and might take several time to be manually corrected). In the case of satellite imagery (as for the Milan study site), the viewing angle is constant for the entire scene. Accordingly, in such circumstance, to properly account for the abovementioned shift we perform different analyses based on the height of the buildings. In particular, we first analyze the only buildings with height lower than 10m (for which the outlines are fitting perfectly). Next, we solely take into account the buildings whose height is between 10 and 20m and shift the CIR

imagery so that it matches the corresponding outlines. Then, we do the same for the buildings with height from 20 to 30m and so on up to when all the buildings matching the flat roof criteria are analyzed. In the case of airborne data, different stripes are acquired separately and then properly mosaicked. However, the buildings far from the center of each acquisition stripe might exhibit a shift with respect to the corresponding outlines (which depends on the swath width). Once combined together all the stripes, there is no systematic means for properly shifting the CIR imagery as done for the satellite data. Typically, the swath width is rather small, hence the effects are limited.

Tree coverage: often one-two story houses in residential areas have gardens with trees even higher than the neighboring building. Sometimes, it might occur that their crown covers partly or even entirely the building roof hence forbidding a correct green roof analysis and resulting in overestimations. This issue is rather challenging and can be solved only during the visual check in the post-processing.

Despite these drawbacks intrinsic to specific data, the developed methods allowed to obtained very accurate products, which have already started being used by the municipalities involved in the DECUMANUs project. Moreover, once finalized the algorithm implementation, it was possible to generate them solely in few days of work, which represent just a very small fraction of the time that would be needed by means of in situ surveys or pure photointerpretation.

6   REFERENCES

ANSEL, W., & Appl, R.: Green Roofs - Bringing Nature Back to Town, Proceedings of the International Green Roof Congress 2009, International Green Roof Association – IGRA. Berlin, 2009.

ANSEL, W., & Diem, A.: Integrated Rainwater Management with Green Roof – Building Site "Hohlgrabenäcker" in Stuttgart Zuffenhausen, Green Roofs. In: Bringing Nature Back to Town, Proceedings of the International Green Roof Congress 2009, International Green Roof Association – IGRA, pp. 149-152. Berlin, 2009.

BERNDTSSON, J. C.: Green Roof performance towards management of runoff water quantity and quality: A review. In: Ecological Engineering, Vol. 36, Issue 4, pp. 351-360. 2010.

GALL, H., Schuster, D., Jafvert, C., & Rhoads, W.: Design, Implementation, and Monitoring of Purdue's first Green Roof. In: Proceedings of the International High Performance Building Conference, Purdue University. Purdue, 2010.

GSCHWANTNER, T., Vidal, K., Lanz, A., Tomppo, E., Di Cosmo, L., Robert, N., Englert Duursma, D., & Lawrence, M.: Common tree definitions for national forest inventories in Europe. In: Silva Fennica, Vol. 43, Issue 2, pp. 303–321. 2009.

HERMAN, R.: Greenroofs in Germany: yesterday, today and tomorrow. In: Greening Rooftops for Sustainable Communities, pp. 41-45. Chicago, 2003.

HUI, S. C. M.: Study of Thermal and Energy Performance of Greenroof Systems, Department of Mechanical Engineering. The University of Hong Kong. 2009.

KARLSON, M., Reese, H., & Ostwald, M.: Tree Crown Mapping in Managed Woodlands (Parklands) of Semi-Arid West Africa Using WorldView-2 Imagery and Geographic Object Based Image Analysis. In: Sensors, Vol. 14, Issue 12, pp. 22643-22669. 2014.

LIU, K, & Baskaran, B.: Thermal Performance of green roofs through field evaluation. In: Proceedings of the First North American Green Roof Infrastructure Conference, Awards and Trade Show. Chicago, 2014.

THMARCONCINI, M., Metz, A., Zeidler, J., & Esch, T.: Urban Monitoring in Support of Sustainable Cities. In: Proceedings of the 2015 Joint Urban Remote Sensing Event (JURSE). Lausanne, 2015.

OBERNDORFER, E., Lundholm, J., Bass, B., Coffman, R., Doshi, H., Dunnett, N., Gaffin, S., Köhler, M., Liu, K., & Rowe, B.: Green Roofs as Urban Ecosystems: Ecological Structures, Functions, and Services. In: BioScience, Vol. 57, Issue 10, pp. 823-833. 2007.

PECK, S. W., Kuhn, M. E., & Bass, B.: Greenbacks from Green Roofs: Forging a New Industry in Canada. Status Report on Benefits, Barriers and Opportunities for Green Roof and Vertical Garden Technology Diffusion. 1999.

ROUSE, J.W, Haas, R.H., Scheel, J.A., & Deering, D.W.: Monitoring Vegetation Systems in the Great Plains with ERTS. In: Proceedings of the 3rd Earth Resource Technology Satellite (ERTS) Symposium, Vol. 1, pp. 48-62. 1974.

ROWE, D. B.: Green Roofs as a means of pollution abatement. In: Environmental Pollution, Vol. 159, Issue 8-9, pp. 2100-2110. 2011.

VANWOERT, N., Rowe, D., Jeffrey, A., Rugh, C., Fernandez, R., & Xiao, L.: Green Roof Stormwater Runoff Retention: Effects of Roof Surface, Slope, and Media Depth. In: Journal of Environmental Quality, Vol. 34, Issue 3, pp. 1036-1044. 2005.

YANG, J., Yu, Q., & Gong, P.: Quantifying air pollution removal by green roofs in Chicago. In: Atmospheric Environment, Vol. 42, Issue 31, pp. 7266-7273. 2008.

ZEIDLER, J., Esch, T., & Ansel, W.: Fernerkundliche Inventarisierung und Potenzialanalyse von Dachbegrünung - Benutzerhandbuch Software (in press). 2015.